0026-895X/02/6205-1128–1136$7.00
MOLECULAR PHARMACOLOGY
Copyright © 2002 The American Society for Pharmacology and Experimental Therapeutics
Mol Pharmacol 62:1128–1136, 2002

Vol. 62, No. 5
1806/1017639
Printed in U.S.A.

Interaction of the Metal Chelator 2,3-Dimercapto-1-propanesulfonate with the Rabbit Multispecific Organic Anion Transporter 1 (rbOAT1)

A. BAHN, M. KNABE, Y. HAGOS, M. RÖDIGER, S. GODEHARDT, D. S. GRABER-NEUFELD, K. K. EVANS, G. BURCKHARDT, and S. H. WRIGHT

Zentrum für Physiologie und Pathophysiologie, Abt. Vegetative Physiologie, Universität Göttingen, Göttingen, Germany (A.B., M.K., Y.H., M.R., S.G., G.B.); Department of Physiology, College of Medicine, University of Arizona, Tucson, Arizona (D.S.G., K.K.E., S.H.W.)

Received April 18, 2002; accepted July 30, 2002

This article is available online at http://molpharm.aspetjournals.org

ABSTRACT

The metal chelator DMPS (2,3-dimercapto-1-propanesulfonate) is used to treat heavy metal intoxication because it increases renal excretion of these toxins, which are accumulated in proximal tubule cells. To evaluate the involvement of the organic anion transporter 1 (OAT1) in the renal flux of DMPS, we examined the effect of DMPS on transport mediated by the rabbit ortholog of OAT1 and compared these characteristics with those observed in intact isolated rabbit proximal tubules. The rabbit OAT1 (rbOAT1) cDNA consisted of 2124 base pairs encoding a protein of 551 amino acids. Heterologous expression in COS-7 cells revealed rbOAT1-mediated transport of *p*-aminohippurate (PAH; K_t = 16 μM). A 1 mM concentration of unlabeled PAH, α-ketoglutarate, urate, or probenecid inhibited [^{3}H]PAH uptake by 70 to 90%. *cis*-Inhibition and *trans*-stimulation experiments using several Krebs cycle intermediates implicated α-ketoglutarate as the main intracellular exchange anion. Reduced DMPS inhibited rbOAT1-mediated fluorescein transport with an apparent K_i of 102 μM. These characteristics paralleled those observed in isolated rabbit proximal tubules. PAH was transported into nonperfused single proximal tubule S_2 segments with a K_t of 76 μM. DMPS inhibited FL uptake into single tubule segments with a $K_{i\text{-app}}$ of 71 μM. Fluorescein efflux from preloaded tubules was *trans*-stimulated by 1 mM PAH and 1 mM DMPS, consistent with DMPS entry into tubule cells by rbOAT1. In summary, rbOAT1 mediates basolateral uptake of DMPS into proximal tubule cells, implicating this process in the detoxification process of heavy metals in the kidneys.

An important task of renal proximal tubules is the secretion of endogenous and exogenous metabolic products and water-soluble xenobiotics. Consequently, the kidney is a main site for the excretion of many drugs, leading in some cases to nephrotoxicity (Burckhardt and Wolff, 2000; Dresser et al., 2001). A substantial fraction of such compounds carries a net negative charge at physiological pH and hence are referred to as organic anions (OAs). *p*-Aminohippurate (PAH) is the prototypic substrate for what is frequently referred to as the "classic" process of renal organic anion secretion (Pritchard and Miller, 1993). Recently, two PAH-transporters [organic anion transporter (OAT) 1 and OAT3] were identified and functionally characterized on the molecular level (Sekine et al., 1997; Sweet et al., 1997; Reid et al., 1998; Kusuhara et al., 1999; Cha et al., 2001). The overlapping substrate specificity and localization at the basolateral membrane of renal proximal tubules (Tojo et al., 1999; Cha et al., 2001) supports the assumption that both transport proteins may play a role in the secretion of PAH and other OAs.

The kidney is also a site for accumulation of toxic heavy metals, including mercury, cadmium, and arsenic (Welborn et al., 1998). Several mechanisms have been proposed for the entry of these toxins, especially mercury, into the proximal tubule cell (Zalups, 2000). An established therapy for the reduction of the renal burden of heavy metals is the treatment of patients with 2,3-dimercapto-1-propanesulfonic acid (DMPS; Dimaval). Under physiological conditions, this organic anion efficiently mobilizes mercury in the kidneys with comparatively low toxicity (Aposhian et al., 1995). An investigation on the transport, disposition, and toxicity of inorganic mercury in the presence of DMPS was performed on isolated perfused segments of rabbit proximal tubules (Zalups et al., 1998). The authors reported that exposing tubules preloaded with mercury to a bathing solution containing DMPS resulted in clearance of the mercury from the cells into the luminal filtrate. This effect was blocked by adding

This work was supported by National Institutes of Health grants DK56224 and ES04940.

ABBREVIATIONS: OA, organic anion; PAH, *p*-aminohippuric acid; OAT, organic anion transporter; DMPS, 2,3-dimercapto-1-propanesulfonic acid; TEA, tetraethylammonium; RT, reverse transcription; PCR, polymerase chain reaction; RACE, rapid amplification of cDNA ends; FL, fluorescein; rbOAT1, rabbit ortholog of the organic anion transporter 1; bp, base pair(s); ORF, open reading frame; UTR, untranslated region.

PAH to the DMPS-containing bath, implicating OA transport as a means of entry of the chelator into the cells. However, because PAH is known to interact with multiple basolateral transporters in proximal cells, the molecular mode of operation of DMPS in proximal tubule cells that finally leads to a chelation and rapid excretion of heavy metals is still far from clear.

DMPS has been shown to interact with the human ortholog of OAT1. Islinger et al. (2001) showed that hOAT1 has comparatively high affinities for both reduced DMPS (K_i of 22.4 μM) and oxidized DMPS (K_i of 66 μM). They also demonstrated that DMPS can *trans*-stimulate PAH flux across cells expressing hOAT1, suggesting that the transporter accepts the chelator as a substrate. However, evidence integrating the activity of the cloned transporter with that occurring in physiologically intact renal tubules has been lacking. The present report has a 2-fold purpose. First, we report the cloning and functional characterization of the rabbit ortholog of OAT1, enabling comparison of the anion-transporting activity of this cloned transporter with that seen in physiologically intact, isolated renal proximal tubules. Second, to extend the functional comparison of a cloned transporter with activity in the native tubule, we characterize the interaction of DMPS with rbOAT1 and with single isolated rabbit proximal tubules. The results support the conclusion that OAT1 represents an important avenue of DMPS entry into renal cells.

Materials and Methods

Materials. Materials used included fetal bovine serum, trypsin, phosphate-buffered saline from Invitrogen (Groningen, the Netherlands), buffer ingredients, unlabeled substrates, such as PAH, tetraethylammonium (TEA), α-ketoglutarate, DMPS, malate, fumarate, succinate, citrate, oxalacetate, urate, pyruvate, and probenecid (Sigma-Aldrich, Deisenhofen, Germany), and fluorescein from Molecular Probes (Leiden, Netherlands). [^{3}H]PAH (3.25 Ci/mmol) was purchased from PerkinElmer Life Sciences (Boston, MA).

Total RNA Extraction and RT-PCR. Approximately 100 mg of rabbit renal cortical tissue was homogenized with a mortar and pestle in liquid nitrogen and transferred to the extraction buffer of the RNeasy total RNA extraction kit (QIAGEN, Hilden, Germany). Total RNA was extracted according to the manufacturer's protocol. One microgram of this RNA was used for reverse transcription with omniscript reverse transcriptase (QIAGEN) and an oligo(dT)-anchor primer [5′-GACCACGCGTATCGATGTCGAC $(T)_{18}$(AGC)-3′] at 37°C for 1 h. Four microliters of the RT reaction was taken for a standard PCR (94°C for 2 min, 94°C for 30 s, 55°C for 30 s, 72°C for 1 min, for 35 cycles) with degenerate primers (sense primer, 5′ CCTCYTTCAACTGCATCTTCCTG 3′; antisense primer, 5′ CTTCTCTTGTGYTGAGGCCTG 3′). After visualization of the PCR product in an agarose gel by ethidium bromide, it was cut out of the gel, extracted with the Nucleotrap-kit (Macherey and Nagel, Düren, Germany) and subcloned into the pUC57-plasmid (MBI Fermentas, St. Leon-Rot, Germany). Positive clones were screened by standard PCR with plasmid primers (M13 universe/reverse). To amplify the entire rbOAT1-ORF, 4 μl of an RT-reaction was taken for a standard PCR using 1.2 units of the proofreading polymerase powerscript (PAN Biotech, Aidenbach, Germany) and specific primers (sense primer, 5′-GAAGATCTATGGCCTTCAATG-3′; antisense primer, 5′-GATCTAGATCAGAGTCCATTC-3′). The primers were constructed from sequence information using 5′- and 3′-RACE. The PCR product was cloned into pcDNA3.1 with the TOPO-pcDNA3.1 cloning kit (Invitrogen, Groningen, Netherlands).

5′- and 3′-RACE. The RT of the kidney total RNA was purified with the High Pure PCR purification kit (Roche Applied Science, Mannheim, Germany) and eluted in 25 μl of H_2O, pH 8.0. A part of this purified RT was used for a 5′-tailing reaction with 25 mM dATP and 30 units of a terminal transferase (Invitrogen) for 1.5 h at 37°C. 5′-RACE was performed with a specific OAT1 primer derived from the human sequence (antisense, 5′-CAGTGTCATGCAGTTGAG-3′) to anneal within the first part of the open reading frame. An oligo(dT)-anchor primer was taken in the first PCR and a RACE primer (5′ GACCACGCGTATCGATGTCGAC 3′) was used in the second ("nested") PCR, applying 1.2 units of powerscript polymerase (PAN Biotech, Aidenbach, Germany) at 55°C annealing temperature. The 3′-RACE was carried out from the same purified RT with a specific OAT1 forward primer (5′-CTGGGACAGCCTCTACCG-3′) and the RACE primer. The resulting PCR-products were cloned with the TOPO-XL-cloning kit (Invitrogen, Groningen, Netherlands).

Sequencing. Positive clones were sequenced with different synthesized oligonucleotide primers derived from the hOAT1-cDNA and rbOAT1 by the dye-termination method using an automatic sequencer (ABI 377; Applied Biosystems, Weiterstadt, Germany). Sequence analysis was performed with several online services [e.g., CAP3 (http://pbil.univ-lyon1.fr/cap3.html), MAP (http://genome.cs.mtu.edu/map.html), FASTA (http://www.ebi.ac.uk/fasta33/)].

Cell Culture and Uptake Experiments. The monkey kidney cell line COS-7 was cultivated in plastic flasks or Petri dishes (Sarstedt, Nümbrecht, Germany) in Dulbecco's modified Eagle's medium (Invitrogen) with 580 mg/l glutamine, 110 mg/l Na-pyruvate and with 10% heat-inactivated fetal calf serum in 8.5% CO_2 at 37°C. Five micrograms of rbOAT1-pcDNA3.1 construct was transiently transfected into COS-7 cells by electroporation (GenePulser II; Bio-Rad, München, Germany) at 250 V and 300 μF. Twenty-four hours after transfection, the cells were plated in six-well plastic dishes (Sarstedt) at a density of 2×10^5 cells/well. Transport assays were performed 48 h after transfection in buffer (110 mM NaCl, 3 mM KCl, 1 mM $CaCl_2$, 0.5 mM $MgSO_4$, 1 mM KH_2PO_4, 10 mM HEPES, and 5 mM glucose, pH 7.5). In the *trans*-stimulation experiments, the cells were preloaded for 2 to 3 h with each of the tested substances. The cells were washed twice with buffer and incubated at room temperature in buffer containing 1 μM fluorescein (FL) or 0.2 μM [^{3}H]PAH. In some cases, the test solutions also included additional test substances (as described in the figure legends). The incubation was stopped and the extracellular tracer was removed by washing the monolayer two to three times with ice-cold phosphate-buffered saline. Cells were dissolved in 0.5 to 1 ml of 0.5 N NaOH. To assess FL accumulation, fluorescence was measured in a fluorescence spectrophotometer (Hitachi, Tokyo, Japan) at 492/512 nm (excitation/emission). [^{3}H]PAH content was determined by scintillation counting (Canberra-Packard, Dreieich, Germany). The protein content of each well was determined according to the Bradford (1976) procedure.

Preparation of Intact S_2 Segments of Rabbit Kidney Cortex and Flux Measurements. S_2 segments of proximal tubules, ~1.5 mm in length, were isolated from kidneys of New Zealand White rabbits (Myrtle's Rabbitry, Thompson Station, TN) applying previously published methods (Welborn et al., 1998). Tubules were dissected in the lid of a plastic Petri dish that was kept on ice and contained dissection buffer (110 mM NaCl, 25 mM $NaHCO_3$, 5 mM KCl, 2 mM Na_2HPO_4, 1.8 mM $CaCl_2$, 1 mM $MgSO_4$, 10 mM sodium acetate, 8.3 mM D-glucose, 5 mM L-alanine, 4 mM lactate, and 0.9 mM glycine, adjusted to pH 7.4 with HCl or NaOH, and gassed continuously with 95% O_2/5% CO_2 to maintain the pH; osmolality was ~290 mOsmol/kg H_2O). Segments of proximal tubules were individually dissected from the cortical zone and a segment was transferred to a glass-bottomed aluminum superfusion chamber containing superfusion buffer. The chamber was transferred to the stage of an Olympus IMT microscope and superfused with buffer at 5 ml/min. The chamber was water-jacketed and its temperature, as well as that of the incoming superfusion buffers, was maintained at

37°C. Superfusion buffers could be changed in a few seconds while maintaining a constant flow rate and temperature. A small vacuum line on the side of the chamber removed overflow.

Measurements of FL uptake into isolated proximal tubules were performed using the technique of Welborn et al. (1998). Tubules were observed with an Olympus IMT microscope equipped with a 40× oil-immersion fluor objective (1.3 numerical aperture; Nikon, Tokyo, Japan). Excitation light (490 nm) from a 75-W xenon lamp coupled with a monochromator (Photon Technology International, Brunswick, NJ) was directed on the tubule section with a 490-nm dichroic mirror (model 490DCLP; Omega Optical, Brattleboro, VT). Emitted light (collected as photons per second) was measured at 1-s intervals using a photomultiplier tube (model HC120; Hamamatsu, Bridgewater, NJ) coupled to a 520-nm long-pass filter (Omega Optical). The signal from tubule autofluorescence at this wavelength was <1% of the signal arising from exposure to 1 μM FL (Welborn et al., 1998).

All tests for FL uptake into intact tubules were performed at an external concentration of 1 μM. Data from the first 5 to 7 s after the shift from control buffer to buffer containing FL was ignored (owing to the exchange kinetics of the chamber solution), and the rate of FL uptake was calculated by linear regression of the next 30-s period representing the initial rate. After exposure to FL, the superfusion solution was shifted to a FL-free bath and FL was allowed to clear from the tubule for 10 min (sufficient to return to within a few percentage points of background), after which another uptake trial could be performed. A single tubule could usually be used for a period of >2 h, which allowed for multiple uptake trials. [^{3}H]PAH uptake into intact tubules was studied using 5 μM [^{3}H]PAH over an incubation period of 15 s.

FL efflux was measured by loading tubules for a longer period, usually 60 s, and then monitoring the decrease in tubule fluorescence over a 90-s period after exposure to a FL-free medium. Efflux data are expressed as percentage of fluorescence measured at time 0 (when FL efflux commenced). Because tubules were loaded for a longer period, the intervals between trails were also lengthened (to approximately 20 min) to permit accumulated FL to washout from the tubule.

Kinetic and Statistical Analysis. Unless indicated otherwise, data are the mean (± S.E.) of three independent experiments with three repeats each. Kinetic constants were calculated using SigmaPlot 2001 (SPSS Science, Chicago, IL).

Results

Cloning of Rabbit Organic Anion Transporter 1 (rbOAT1). Cloning the rabbit ortholog of OAT1 (rbOAT1) started with a reverse transcription of total RNA extracted out of rabbit kidney cortex. A PCR approach, using degenerate primers derived from the human and rat cDNA sequences, was performed yielding a rabbit-specific 350-bp fragment (data not shown). To complete the ORF and parts of the untranslated regions (UTR), 5′ and 3′ RACEs were carried out. The RACE products were subcloned into TOPO-XL plasmid and sequenced. This resulted in the final cDNA sequence that consisted of a 1656-bp ORF coding for 551 amino acids and the complete 5′ and 3′ UTR region with 278 and 190 bp, respectively.[1] A sequence alignment (Fig. 1) with the known OAT1 orthologs showed a high identity of rbOAT1 to the human (89%), rat (88%), pig (87%), and mouse (85%) OAT1 proteins. Further studies of the expression of rbOAT1 in kidney using OAT1-specific primers and a RACE reverse primer revealed an alternative OAT1-specific 3′ UTR product of 874 bp (data not shown), illustrating that OAT1 is alternatively spliced in the kidney. ScanProsite analysis (http://us.expasy.org/tools/scanprosite/; Fig. 2) for putative phosphorylation sites resulted in five protein kinase C phosphorylation sites at positions 129, 190, 271, 284, and 521, including three highly conserved positions, and five casein kinase II phosphorylation sites at positions 83, 122, 325, 515, and 544. Consistent with the other OAT1 orthologs, analysis (TopPred2; http://bioweb.pasteur.fr/seqanal/interfaces/toppred.html) of the rbOAT1 sequence suggested the presence of twelve putative transmembrane spanning domains.

Functional Characterization of rbOAT1. Fig. 3 shows the time course of [^{3}H]PAH uptake into COS-7 cells transiently transfected with the cDNA for rbOAT1. Substrate accumulation increased with time for at least 10 min, and 2-min incubations were used in subsequent experiments to provide estimates of the initial rate of transport of [^{3}H]PAH. Figure 4 shows the effect of increasing concentrations of unlabeled PAH on the uptake of [^{3}H]PAH into either wild-type COS-7 cells or cells transfected with rbOAT1. In the absence of unlabeled PAH (which competitively blocks transport of the labeled substrate), uptake of [^{3}H]PAH into cells transfected with rbOAT1 was increased 10-fold over that measured in the nontransfected cells. Whereas addition of unlabeled PAH profoundly inhibited uptake of [^{3}H]PAH into the rbOAT1 cells, the unlabeled substrate had virtually no effect on transport into the wild type cells. The rbOAT1-specific uptake of PAH (i.e., transport in transfected cells minus that observed in nontransfected cells) was a saturable function of substrate concentration that was adequately described by the Michaelis-Menten equation for competitive interaction of labeled and nonlabeled substrate (Malo and Berteloot, 1991):

$$J = \frac{J_{max}[*PAH]}{K_t + [*PAH] + [PAH]} + C \quad (1)$$

where J is the rate of [^{3}H]PAH transport from a concentration of labeled substrate equal to [*PAH], J_{max} is the maximum rate of mediated PAH transport, K_t is the PAH concentration that results in half-maximal transport (Michaelis constant), [PAH] is the concentration of unlabeled PAH in the transport reaction, and C is a constant that represents the component of total PAH uptake that is not saturated (over the range of substrate concentrations tested) and presumably reflects the combined influence of diffusive flux, nonspecific binding and/or incomplete rinsing of the cell layer. Data from three separate experiments resulted in a calculated value for apparent K_t of 15.6 μM, with a J_{max} of 157 pmol/mg of protein/2 min (Fig. 4).

The substrate specificity of rbOAT1 was further studied by comparing the effect on [^{3}H]PAH uptake of 1 mM of concentrations of unlabeled PAH, probenecid, α-ketoglutarate, urate, or TEA. All tested substances reduced [^{3}H]PAH uptake by 70 to 90%, except the cationic substance TEA, which showed no effect (Fig. 5). In situ, OAT1 supports concentrative accumulation of exogenous anions through exchange with endogenous intracellular dicarboxylates such as α-ketoglutarate (Sekine et al., 1997; Sweet et al., 1997). Therefore, the anion selectivity of rbOAT1 was examined by measuring *cis*-inhibition produced by 1 mM concentrations of PAH, probenecid, pyruvate, citrate, α-ketoglutarate, succinate, fuma-

[1] The nucleotide sequence reported in this article has been submitted to EMBL/GenBank with accession number AJ242871.

rate, malate, and oxalacetate (Fig. 6A) or *trans*-stimulation induced by 1 mM preload with PAH, urate, pyruvate, citrate, glutarate, α-ketoglutarate, succinate, fumarate, malate, and oxalacetate (Fig. 6B). Except for glutarate, α-ketoglurate, urate, and PAH, none of these substances had an effect on rbOAT1-mediated transport of fluorescein.

Influence of Reduced DMPS on FL Uptake by rbOAT1 Compared with PAH. Intact tubules also accumulate FL by a process with the physiological characteristics of OAT1, including inhibition by PAH and probenecid (Sullivan et al., 1990) and *trans*-stimulation by oppositely oriented gradients of α-ketoglutarate (Welborn et al., 1998) and glut-

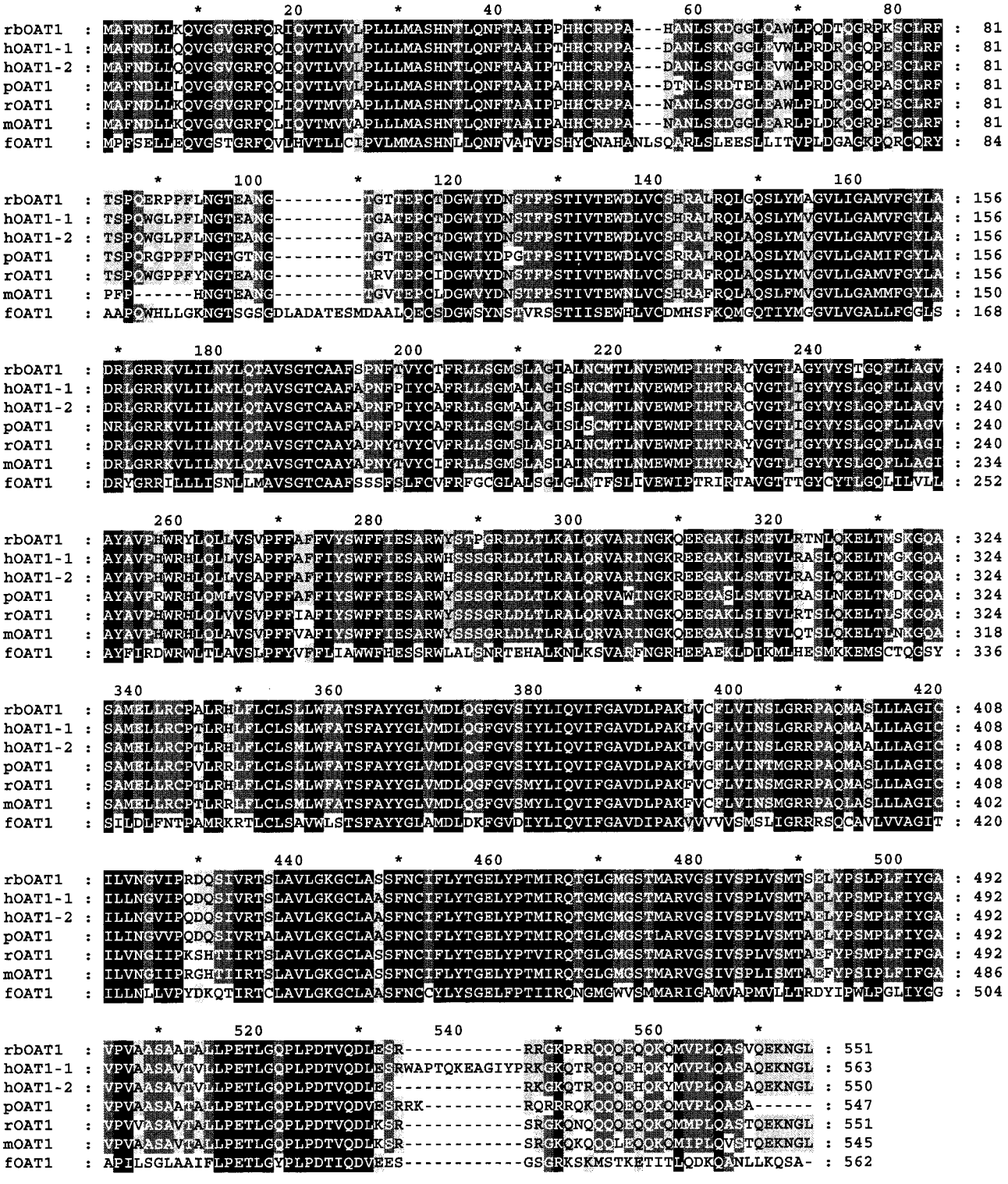

Fig. 1. Amino acid sequence of rbOAT1 aligned with human OAT1 isoform 1 (hOAT1–1) and isoform 2 (hOAT1–2), pig OAT1 (pOAT1), rat OAT1 (rOAT1), mouse OAT1 (mOAT1), and flounder OAT1 (fOAT1). White-on-black residues indicate 100% identity, white-on-dark gray residues indicate 80% identity, and black-on-light gray residues indicate 60% identity.

arate (Sullivan and Grantham, 1992). *trans*-Stimulation studies with cells preloaded with 1 mM PAH revealed that PAH is able to drive FL uptake 1.6-fold over control, demonstrating that rbOAT1 supports PAH/FL exchange (Fig. 6B). FL is commonly used as a test substrate of OA transport in intact tubules (Sullivan et al., 1990; Welborn et al., 1998), including experiments described in an upcoming section of the present report. Consequently, we characterized the interaction of PAH and DMPS with rbOAT1-mediated FL transport. PAH inhibition of FL transport was adequately described by the kinetics of competitive inhibition, according to the relationship (Groves et al., 1998):

$$J = \frac{J_{\text{m-app}}[S]}{K_{\text{i-app}} + [I]} + C \quad (2)$$

where J is the rate of substrate transport (e.g., FL) from a concentration of [S], $J_{\text{m-app}}$ is a constant equal to the maximal rate of substrate transport times K_i/K_t (where K_i is the competitive inhibitor constant for the inhibitor I; K_t is the Michaelis constant for transport of S), $K_{\text{i-app}}$ is an apparent inhibitor constant equal to K_i (1 + [S]/K_t), [I] is the concentration of inhibitor, and C is a constant that represents the component of total substrate uptake that is not saturated (over the range of inhibitor concentrations tested). The $K_{\text{i-app}}$ for PAH was 39 μM (Fig. 7A). Inhibition of FL transport by DMPS was also adequately described by eq. 2, with a $K_{\text{i-app}}$ of 102 μM (Fig. 7B).

Peritubular OA Transport in Isolated S_2 Segments of Rabbit Renal Proximal Tubules—Interaction with DMPS. Peritubular PAH transport is generally acknowledged as reflecting, at least in part, activity of OAT1 in the intact tubule. Consequently, we first confirmed the characteristics of peritubular PAH transport into S_2 segments of rabbit proximal tubule. This transport was saturable, with a K_t of 75.8 ± 20.5 μM and a J_{max} of 6.7 ± 2.3 pmol/mm/min (Fig. 8). Application of 1 mM TEA had no effect on this transport (Fig. 9). We tested the degree to which reduced DMPS interacts with rabbit OAT1, as expressed in the native tubule, by gauging its effect on FL uptake and efflux in single, isolated S_2 segments of rabbit proximal tubule. The initial rate of FL accumulation into single tubules was inhibited by increasing concentrations of reduced DMPS with a $K_{\text{i-app}}$ of 71 μM (Fig. 10). To obtain evidence that DMPS can serve as a transported substrate of basolateral rbOAT1 in intact tubules, we examined the effect of *trans*-substrate gradients on efflux of FL from preloaded tubules. Figure 11A shows that an inwardly directed PAH gradient resulted in a marked stimulation in the basolateral efflux of FL from single proximal tubules. At 60 s, addition of 1 mM PAH in the superfusate increased FL efflux by 84% compared with control efflux measured in the absence of an exogenous organic anion. When 1 mM DMPS was added to the superfusate, FL efflux was also stimulated (Fig. 11B), with efflux at 60 s being increased by 41% over the parallel control efflux. These data are consistent with the conclusion that reduced DMPS can both bind to and be transported by rbOAT1.

Discussion

Renal OA secretion arises from peritubular and luminal transport processes arranged in series. Although the luminal efflux step remains poorly characterized, the peritubular transport processes, which involves uptake from the blood into proximal tubule cells, has received extensive study. Indeed, it is generally viewed as both the active and rate-limiting step in tubular OA secretion (Pritchard and Miller, 1993). Peritubular transport of PAH and other OAs (including fluorescein) has been used to characterize what is frequently referred to as the "classic" renal OA transport pathway. The physiological hallmarks of this process include its marked selectivity of OAs over other structural classes of compounds, and catalysis of the mediated exchange of selected dicarboxylates (e.g., glutarate and α-ketoglutarate) for PAH and other OAs. OAT1 shares both of these general characteristics, leading to the speculation that OAT1 is the molecular identity of the classical pathway (Sekine et al.,

species	Identity with rbOAT1 in % (amino acids)	Protein kinase C phosphorylation sites						Casein kinase II phosphorylation sites				
		consensus					non-consensus	consensus				non-consensus
		1	2	3	4	5		1	2	3	4	
rbOAT1 (551 aa)	100	Ser129	Ser271	—	Thr284	—	Thr190, Ser521	Thr122	Ser325	Thr515	Ser544	Ser83
hOAT1-1 (563 aa)	87.74	Ser129	Ser271	Ser278	Thr284	Thr334	—	Thr122	Ser325	Thr515	Ser556	Thr526
hOAT1-2 (550 aa)	89.47	Ser129	Ser271	Ser278	Thr284	Thr334	—	Thr122	Ser325	Thr515	Ser543	—
rOAT1 (551 aa)	87.84	Ser129	Ser271	Ser278	Thr284	Thr334	—	—	Ser325	Thr515	Ser544	—
mOAT1 (545 aa)	85.48	Ser123	Ser265	Ser272	Thr278	Thr328	—	—	Ser319	Thr509	Ser538	—
fOAT1 (563 aa)	47.25	—	Ser283	Ser290	—	—	Thr13, Thr126, Ser144, Ser168, Ser324, Thr433, Ser536, Ser543	—	Ser337	Thr527	—	Ser61, Ser543, Thr549

species	Identity with rbOAT1 in % (amino acids)	Tyrosine kinase phosphorylation sites (consensus)	cAMP- and cGMP-dependent protein kinase phosphorylation sites
hOAT1-1 (563aa)	87.74	Tyr549	—
hOAT1-2 (550aa)	89.47	Tyr536	—
fOAT1 (563aa)	47.25	—	Thr351, Ser409

Fig. 2. Comparative ScanProsite analysis of rbOAT1, hOAT1–1, hOAT1–2, rOAT1, mOAT1, and fOAT1 for putative phosphorylation sites.

1997; Sweet et al., 1997). Immunocytochemical localization of rat OAT1 to the basolateral membrane of cells in the S_2 segment of proximal tubule (Tojo et al., 1999) further supports this suggestion, in light of evidence that peritubular PAH transport is greatest in this segment (Shimomura et al., 1981).

Transport in intact proximal tubules reflects the net activity of all associated transport processes. Three related OATs (OAT2, OAT3, and OAT4; Sekine et al., 2000) have been found in the kidney; one of these, OAT3, transports PAH and is highly expressed in the basolateral membrane of proximal tubules (Motohashi et al., 2002). Thus, although it is evident that OAT1 can play an important role in renal OA transport, it is premature to conclude that OAT1 accounts for all peritubular transport associated with OA secretion in the proximal tubule.

Characterization of Rabbit OAT1. The decision to clone the rabbit ortholog of OAT1 was made, in part, to facilitate comparison of the molecular characteristics of OAT1 to the functional characteristics of OA transport in intact renal proximal tubules. Peritubular OA transport has been studied extensively in the rabbit, in large part due to the comparatively unique ability to make measurements in single isolated renal tubules, thereby permitting direct assessment of transport function of defined nephron segments. The general characteristics of rbOAT1-mediated transport reported here matched closely those of other OAT1 orthologs. The K_t for rbOAT1-mediated PAH transport in COS-7 cells was 16 μM (Fig. 4), which is within the range reported for OAT1 orthologs cloned from human (5–10 μM; Hosoyamada et al., 1999; Lu et al., 1999), rat (14–70 μM; Sekine et al., 1997; Sweet et al., 1997), pig (12.4 μM; Y. Hagos, A. Bahn, A. R. Asif, W. Krick, M. Sendler, and G. Burckhardt, submitted), mouse (37–160 μM; Lopez-Nieto et al., 1997; You et al., 2000), and flounder (20–60 μM; Wolff et al., 1997; Burckhardt et al., 2000). rbOAT1 activity was inhibited by an array of OAs, but not by the organic cation TEA (Fig. 5). Preloading rbOAT1-expressing cells with PAH and glutarate *trans*-stimulated uptake of [^{3}H]PAH (compare Figure 6), consistent with the anion exchanger mode of activity routinely observed for OAT1. The absence of a *trans*-effect in cells preloaded with α-ketoglutarate, although somewhat surprising, may well reflect rapid metabolism of this substrate within COS 7 cells.

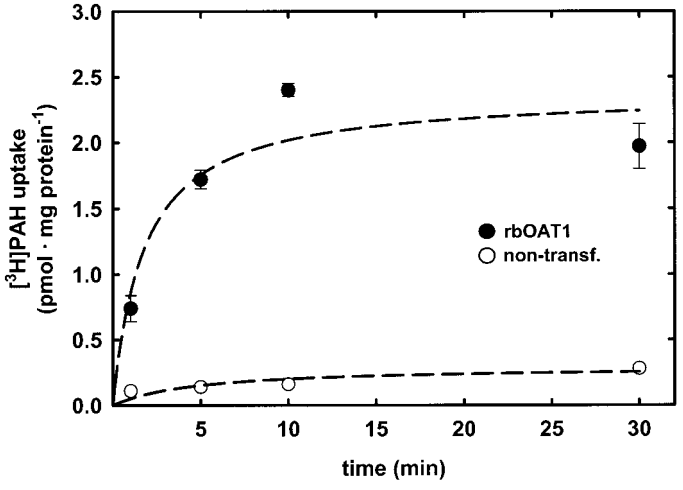

Fig. 3. Time course of [^{3}H]PAH (0.2 μM) uptake into rbOAT1-expressing COS-7 cells and into nontransfected control cells.

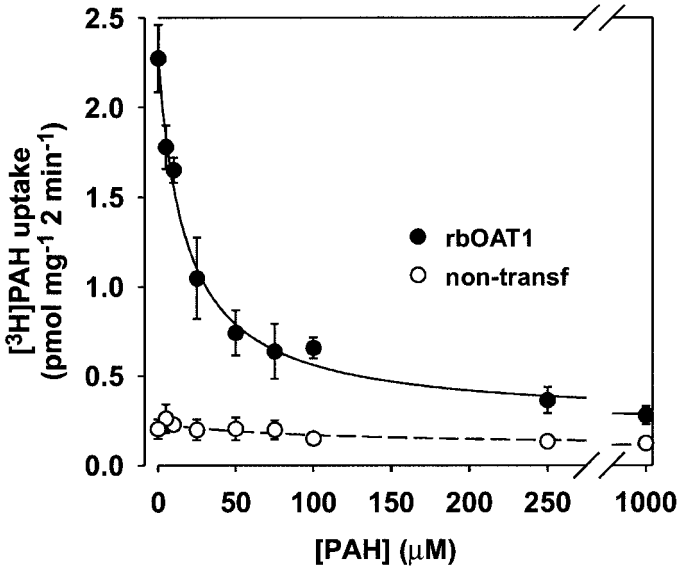

Fig. 4. Effect of unlabeled PAH on the uptake of 0.2 μM [^{3}H]PAH into rbOAT1-expressing COS-7 cells and into nontransfected control cells measured 2 min at RT. The points are the means (± S.E.) of uptakes determined in three separate experiments. The lines were based upon a nonlinear regression algorithm employing eq. 1 (see *Results*).

Comparison of rbOAT1 Activity with OA Transport in Intact Rabbit Proximal Tubules. The study of rbOAT1 permitted quantitative comparisons of the characteristics of a single transporter to those expressed in the native tubule (which may reflect activity of suite of parallel processes). Interestingly, the kinetics of PAH transport in intact tubules and in COS-7 cells transiently transfected with rbOAT1 were rather different. The K_t for PAH transport into nonperfused single proximal tubules measured in the present study was 76 ± 21 μM (n = 5) (Fig. 8), which corresponds reasonably to the value of 108 μM reported in a previous study (Dantzler et al., 1995). K_t values for PAH transport measured in other

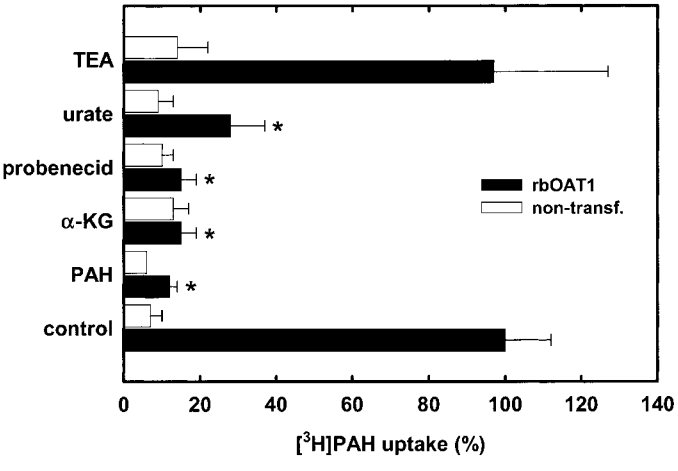

Fig. 5. Inhibition study using several anionic and cationic substances on the uptake of PAH into rbOAT1-expressing COS-7 cells (■). The transport of 0.2 μM [^{3}H]PAH over 2 min incubation time was determined in absence or presence of 1 mM of each of these substances in comparison to nontransfected cells (□). The length of each horizontal column is a mean uptake of two independent transfections with three repeats. Each column is calculated as percentage of radiolabel accumulation under control conditions (100%) measured without inhibitor. *, $p < 0.05$; α-KG, α-ketoglutarate.

preparations of isolated rabbit proximal tubules include 165 μM (tubule suspension; Groves et al., 1998) and 195 μM (for transepithelial secretion in isolated S_2 segments; Shimomura et al., 1981). All of these values are substantially higher than the 16 μM K_t measured for rbOAT1-mediated PAH transport (Fig. 4). There are at least two possible explanations for this discrepancy. The first is that PAH uptake could involve one or more pathways other than OAT1. To this end, it is notable that, in the human cortex, OAT3 and OAT1 are coexpressed in the basolateral membrane of proximal cells, and hOAT3 mRNA expression in cortical tissue is two to three times that of hOAT1 (Motohashi et al., 2002). Also, the K_t for hOAT3-mediated PAH transport is substantially higher than that for hOAT1-mediated transport (~90 μM versus ~5–9 μM, respectively; Hosoyamada et al., 1999; Cha et al., 2001), which correlates with the higher K_t for PAH uptake into tubules compared with rbOAT1-expressing cells. It is remarkable that PAH uptake is markedly reduced into renal slices from OAT3-knockout mice, compared with wild-type littermates (Sweet et al., 2002), implicating OAT3 as a significant contributor to total renal PAH (and organic anion) secretion.

An important caveat needs to be raised here. There are substantial species differences in the kinetic parameters reported for different OAT orthologs; it is possible that rabbit OAT3 could display an affinity for PAH comparable with that observed for rbOAT1. It is also possible, and this is the second potential explanation for the observed discrepancy in PAH kinetics mentioned above, that the quantitative characteristics of rbOAT1 as expressed in COS-7 cells could differ considerably from those expressed in other cell types (e.g., the native renal proximal cell). Thus, comparisons of kinetic parameters of cloned transporters with those measured in native cell systems, although appropriate (indeed, necessary for an understanding of the role individual transporters play in integrated cell physiology), must be interpreted with caution. We suggest it is premature to draw conclusions on the

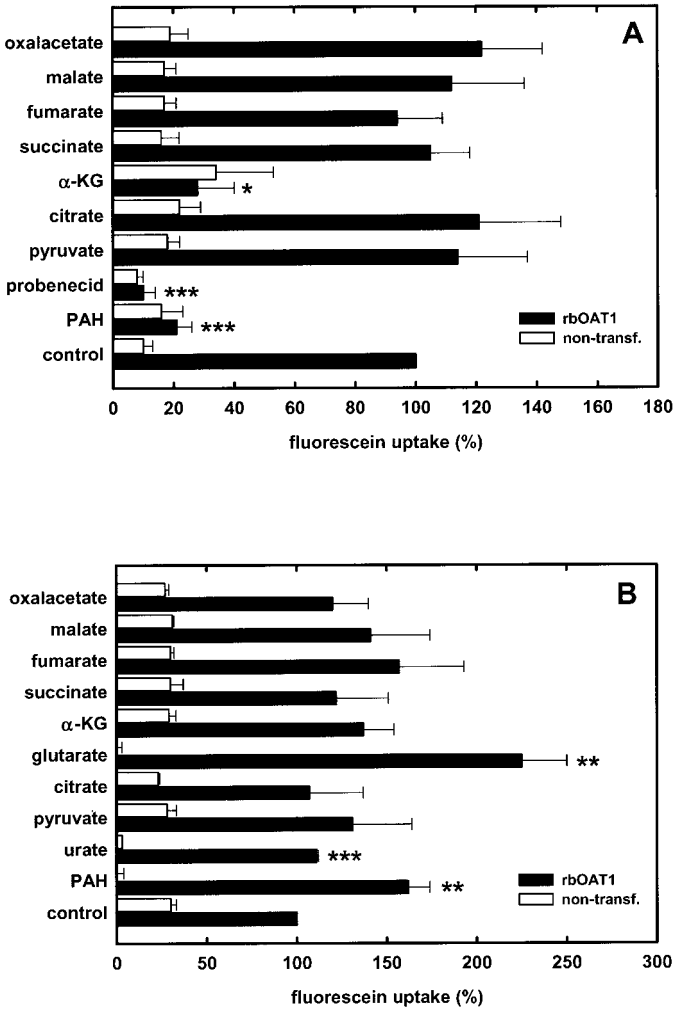

Fig. 6. A, the inhibition of fluorescein uptake on rbOAT1 transfected COS-7 cells (■) was determined using several Krebs cycle intermediates, the classic substrates PAH and α-ketoglutarate (α-KG), and the typical inhibitor probenecid in comparison to nontransfected COS-7 cells (□). Each column is calculated as a percentage of fluorescein accumulation under control conditions (100%) measured without inhibitor (mean ± S.E.M.; n = 3 independent transfections). B, the *trans*-stimulatory potential of several Krebs cycle intermediates as well as of PAH, glutarate, and urate was measured on fluorescein uptake of rbOAT1 transfected COS-7 cells (■) preloaded with 1 mM each for 2 to 3 h. Each column shows the percentage of fluorescein accumulation correlated with the control (100%) measured without *trans*-stimulator (mean ± S.E.M.; n = 3 independent transfections). *, $p < 0.05$; **, $p < 0.01$; ***, $p < 0.001$.

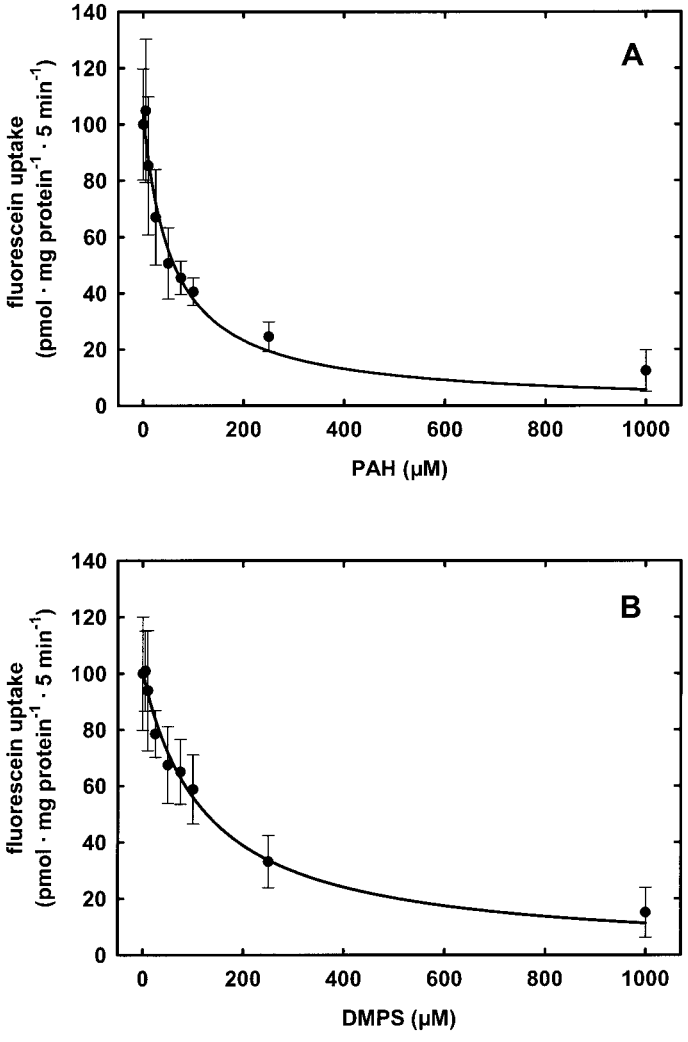

Fig. 7. Kinetics of inhibition of fluorescein uptake into rbOAT1-expressing COS-7 cells by the classic OAT1 substrate PAH (A) and by reduced DMPS (B). The points are the means (± S.E.M.) of uptakes determined in three separate experiments. The lines were based upon a nonlinear regression algorithm using eq. 2 (see *Results*).

source of the discrepancy in measured K_t values in rbOAT1-expressing cells and intact renal tubules. Although it could reflect the activity of multiple transport processes with different affinities for PAH, it could also reflect some combination of technical issues, including the differences associated with cell types and/or physical parameters in different experimental systems.

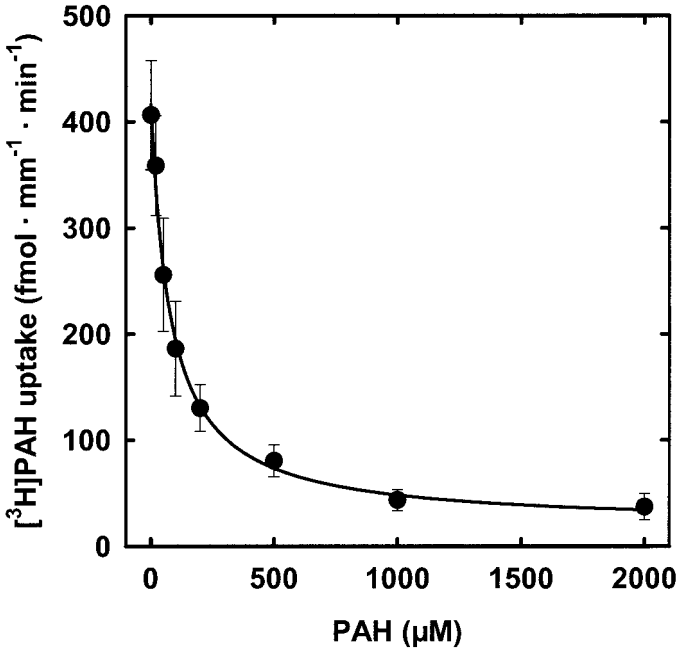

Fig. 8. Kinetics of PAH transport into single isolated S_2 segments of rabbit renal proximal tubule using 5 μM [^{3}H]PAH and an incubation period of 15 s. Each point represents the mean ± S.E. of triplicate measurements from five different experiments (i.e., $n = 5$).

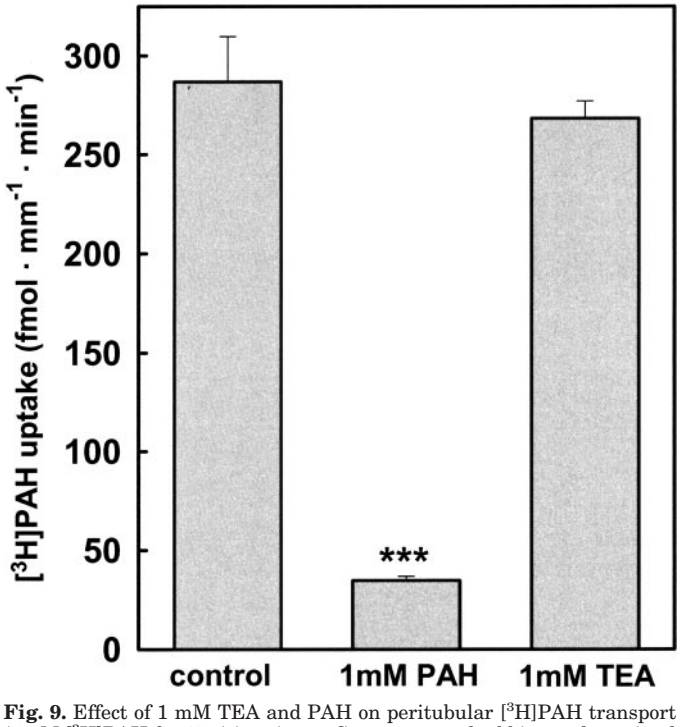

Fig. 9. Effect of 1 mM TEA and PAH on peritubular [^{3}H]PAH transport (5 μM [^{3}H]PAH for 15 s) into intact S_2 segments of rabbit renal proximal tubule. The height of each bar represents the mean ± S.E. of uptakes measured in three separate tubules from the same rabbit ($n = 3$). ***, $p < 0.001$.

Interaction of DMPS with rbOAT1 and Intact Rabbit Proximal Tubules. DMPS applied for several days significantly increases renal heavy metal excretion and reduces the renal burden of heavy metals (Aposhian et al., 1997). The pathways in proximal cells for entry and exit of DMPS and its metal chelates are not clear. However, the principal site of entry of DMPS is likely to be across the basolateral membrane (Zalups, 2000). Because coexposure to PAH or probenecid reduces DMPS-induced clearance of metal from kidneys, the classic OA transport system is believed to play an important role in DMPS entry (Klotzbach and Diamond, 1988; Diamond and Zalups, 1998; Zalups, 2000). Thus, as noted earlier, the presence of multiple OATs in proximal tubule cells underscores the importance of the direct assessment of the interaction of DMPS with these OATs.

Islinger et al. (2001) provided the first evidence that OAT1 is involved in the renal uptake of DMPS. Using the human

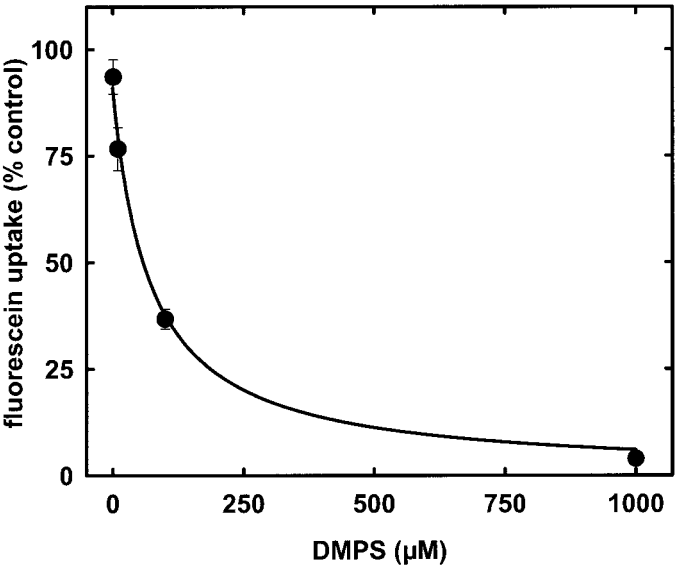

Fig. 10. Kinetics of DMPS inhibition of FL uptake (1 μM FL, 30-s incubation period) into isolated intact S_2 segments of rabbit proximal tubules. Each point represents the mean ± S.E. of measurements made on four tubules from four different animals ($n = 4$).

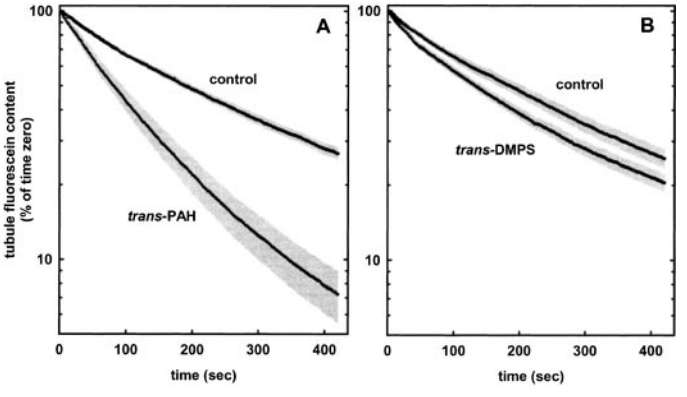

Fig. 11. *trans*-Stimulation study was performed on isolated intact S_2 segments of rabbit kidney cortex. The tubules were preloaded with 0.1 μM fluorescein for 3 min. Providing 1 mM PAH (*trans*-PAH, A) or 1 mM DMPS (*trans*-DMPS, B) continuous efflux of fluorescein was monitored over a period of 420 s. The data are a mean of four tubules from four animals for the PAH kinetic and nine tubules from seven rabbits for the DMPS kinetic. All data were normalized to the level of fluorescence present at time 0. S.D. is shown for each data point.

ortholog of OAT1, they demonstrated an interaction with both reduced and oxidized DMPS (K_i values of 22.4 μM and 66 μM, respectively). They also showed that both forms of DMPS *trans*-stimulate PAH efflux from hOAT1-expressing HeLa cells, supporting the contention that these substances are substrates for OAT1. We extended these observations by comparing the interaction of DMPS with rbOAT1 and with peritubular OA transport in intact rabbit proximal tubules. FL transport mediated by rbOAT1 was inhibited by DMPS with an apparent K_i of 102 μM (Fig. 7B). The similarity between this value and the $K_{i\text{-app}}$ of 71 μM measured in intact rabbit proximal tubules (Fig. 10) is consistent with the conclusion that rbOAT1 plays a significant role in mediating DMPS entry into proximal tubule cells. As expected, and consistent with previous observations, inwardly directed gradients of PAH resulted in a marked *trans*-stimulation of FL efflux from tubules preloaded with the fluorescent substrate (Fig. 11A). A *trans*-gradient of DMPS also stimulated FL transport in intact rabbit tubules, suggesting that DMPS is a transportable substrate of OAT1 in intact proximal tubules (Fig. 11B). The fact that DMPS is a substrate for OAT1 is further underlined by the recent findings of Pombrio et al. (Pombrio et al., 2001). They concluded that selected mercapturic acids serve as high affinity substrates for OAT1.

In summary, we established a "clone/tubule" model system to characterize renal OA transport and the role it can play in DMPS-mediated detoxification of renal heavy metal poisoning. The rabbit ortholog of OAT1 was cloned and showed the same functional characteristics as its human ortholog (hOAT1). rbOAT1 interacted with the heavy metal chelator, DMPS. Comparison with the interaction of DMPS with OA transport in physiologically intact isolated rabbit renal proximal tubules supported the conclusion that rbOAT1 plays a central role in the peritubular entry of DMPS into intact renal proximal tubule cells.

Acknowledgments

We thank A. Hillemann for excellent technical assistance, A. Nolte (Dept. of Biochemistry, Universität Göttingen, Göttingen, Germany) for nucleotide sequencing, and E. Thelen for expert help with the preparation of the illustrations.

References

Aposhian HV, Arroyo A, Cebrian ME, Del Razo LM, Hurlbut KM, Dart RC, Gonzalez-Ramirez D, Kreppel H, Speisky H, Smith A, et al. (1997) DMPS-arsenic challenge test. I: Increased urinary excretion of monomethylarsonic acid in humans given dimercaptopropane sulfonate. *J Pharmacol Exp Ther* **282:**192–200.

Aposhian HV, Maiorino RM, Gonzalez-Ramirez D, Zuniga-Charles M, Xu Z, Hurlbut KM, Junco MP, Dart RC, and Aposhian MM (1995) Mobilization of heavy metals by newer, therapeutically useful chelating agents. *Toxicol* **97:**23–38.

Bradford MM (1976) A rapid and sensitive method for the quantitation of microgram quantities of protein utilizing the principle of protein-dye binding. *Anal Biochem* **72:**248–254.

Burckhardt BC, Wolff NA, and Burckhardt G (2000) Electrophysiologic characterization of an organic anion transporter cloned from winter flounder kidney (fROAT). *J Am Soc Nephrol* **11:**9–17.

Burckhardt G and Wolff NA (2000) Structure of renal organic anion and cation transporters. *Am J Physiol* **278:**F853–F866.

Cha SH, Sekine T, Fukushima JI, Kanai Y, Kobayashi Y, Goya T, and Endou H (2001) Identification and characterization of human organic anion transporter 3 expressing predominantly in the kidney. *Mol Pharmacol* **59:**1277–1286.

Dantzler WH, Evans KK, and Wright SH (1995) Kinetics of interactions of para-aminohippurate, probenecid, cysteine conjugates and *N*-acetyl cysteine conjugates with basolateral organic anion transporter in isolated rabbit proximal renal tubules. *J Pharmacol Exp Ther* **272:**663–672.

Diamond GL and Zalups RK (1998) Understanding renal toxicity of heavy metals. *Toxicol Pathol* **26:**92–103.

Dresser MJ, Leabman MK, and Giacomini KM (2001) Transporters involved in the elimination of drugs in the kidney: organic anion transporters and organic cation transporters. *J Pharm Sci* **90:**397–421.

Groves CE, Morales M, and Wright SH (1998) Peritubular transport of ochratoxin A in rabbit renal proximal tubules. *J Pharmacol Exp Ther* **284:**943–948.

Hosoyamada M, Sekine T, Kanai Y, and Endou H (1999) Molecular cloning and functional expression of a multispecific organic anion transporter from human kidney. *Am J Physiol* **276:**F122–F128.

Islinger F, Gekle M, and Wright SH (2001) Interaction of 2, 3-dimercapto-1-propane sulfonate with the human organic anion transporter hOAT1. *J Pharmacol Exp Ther* **299:**741–747.

Klotzbach JM and Diamond GL (1988) Complexing activity and excretion of 2, 3-dimercapto-1-propane sulfonate in rat kidney. *Am J Physiol* **254:**F871–F878.

Kusuhara H, Sekine T, Utsunomiya-Tate N, Tsuda M, Kojima R, Cha SH, Sugiyama Y, Kanai Y, and Endou H (1999) Molecular cloning and characterization of a new multispecific organic anion transporter from rat brain. *J Biol Chem* **274:**13675–13680.

Lopez-Nieto CE, You G, Bush KT, Barros EJ, Beier DR, and Nigam SK (1997) Molecular cloning and characterization of NKT, a gene product related to the organic cation transporter family that is almost exclusively expressed in the kidney. *J Biol Chem* **272:**6471–6478.

Lu R, Chan BS, and Schuster VL (1999) Cloning of the human kidney PAH transporter: narrow substrate specificity and regulation by protein kinase C. *Am J Physiol* **276:**F295–F303.

Malo C and Berteloot A (1991) Analysis of kinetic data in transport studies: new insights from kinetic studies of Na^+-D-glucose cotransport in human intestinal brush-border membrane vesicles using a fast sampling, rapid filtration apparatus. *J Membrane Biol* **122:**127–141.

Motohashi H, Sakurai Y, Saito H, Masuda S, Urakami Y, Goto M, Fukatsu A, Ogawa O, and Inui K-I (2002) Gene expression levels and immunolocalization of organic anion transporters in the human kidney. *J Am Soc Nephrol* **13**.

Pombrio JM, Giangreco A, Li L, Wempe MF, Anders MW, Sweet DH, Pritchard JB, and Ballatori N (2001) Mercapturic acids (N-acetylcysteine S-conjugates) as endogenous substrates for the renal organic anion transporter-1. *Mol Pharmacol* **60:**1091–1099.

Pritchard JB and Miller DS (1993) Mechanisms mediating renal secretion of organic anions and cations. *Physiol Rev* **73:**765–796.

Reid G, Wolff NA, Dautzenberg FM, and Burckhardt G (1998) Cloning of a human renal *p*-aminohippurate transporter, hROAT1. *Kidney Blood Press Res* **21:**233–237.

Sekine T, Cha SH, and Endou H (2000) The multispecific organic anion transporter (OAT) family. *Pfleug Arch Eur J Physiol* **440:** 337–350

Sekine T, Watanabe N, Hosoyamada M, Kanaim Y, and Endou H (1997) Expression cloning and characterization of a novel multispecific organic anion transporter. *J Biol Chem* **272:**18526–18529.

Shimomura A, Chonko AM, and Grantham JJ (1981) Basis for heterogeneity of *para*-aminohippurate secretion in rabbit proximal tubules. *Am J Physiol* **240:** F430–F436.

Sullivan LP and Grantham JJ (1992) Specificity of basolateral organic anion exchanger in proximal tubule for cellular and extracellular solutes. *J Am Soc Nephrol* **2:**1192–1200.

Sullivan LP, Grantham JA, Rome L, Wallace D, and Grantham JJ (1990) Fluorescein transport in isolated proximal tubules in vitro: epifluorometric analysis. *Am J Physiol* **258:**F46–F51.

Sweet DH, Miller DS, Pritchard JB, Fujiwara Y, Beier DR, and Nigam SK (2002) Impaired organic anion transport in kidney and choroid plexus of organic anion transporter 3 (Oat3 (Slc22a8)) knockout mice. *J Biol Chem* **277:**26934–26943.

Sweet DH, Wolff NA, and Pritchard JB (1997) Expression cloning and characterization of ROAT1: the renal basolateral organic anion transporter in rat kidney. *J Biol Chem* **272:**30088–30095.

Tojo A, Sekine T, Nakajima N, Hosoyamada M, Kanai Y, Kimura K, and Endou H (1999) Immunohistochemical localization of multispecific renal organic anion transporter 1 in rat kidney. *J Am Soc Nephrol* **10:**464–471.

Welborn JR, Shpun S, Dantzler WH, and Wright SH (1998) Effect of α-ketoglutarate on organic anion transport in single rabbit renal proximal tubules. *Am J Physiol* **274:**F165–F174.

Wolff NA, Werner A, Burkhardt S, and Burckhardt G (1997) Expression cloning and characterization of a renal organic anion transporter from winter flounder. *FEBS Lett* **417:**287–291.

You G, Kuze K, Kohanski RA, Amsler K, and Henderson S (2000) Regulation of mOAT-mediated organic anion transport by okadaic acid and protein kinase C in LLC-PK(1) cells. *J Biol Chem* **275:**10278–10284.

Zalups RK (2000) Molecular interactions with mercury in the kidney. *Pharmacol Rev* **52:**113–143.

Zalups RK, Parks LD, Cannon VT, and Barfuss DW (1998) Mechanisms of action of 2,3-dimercaptopropane-1-sulfonate and the transport, disposition and toxicity of inorganic mercury in isolated perfused segments of rabbit proximal tubules. *Mol Pharmacol* **54:**353–363.

Address correspondence to: Dr. Andrew Bahn, Zentrum für Physiologie und Pathophysiologie, Abt. Vegetative Physiologie und Pathophysiologie, Universität Göttingen, Humboldtallee 23, 37073 Göttingen, Germany. E-mail: abahn@veg-physiol.med.uni-goettingen.de